Biological Sciences: Neuroscience

Medin aggregation causes cerebrovascular dysfunction in aging wildtype mice

Karoline Degenhardt[1,2,3,15], Jessica Wagner[1,2,3,15], Angelos Skodras[1,2], Michael Candlish[4], Anna Julia Koppelmann[2,3], Katleen Wild[1], Rusheka Maxwell[2,5], Carola Rotermund[1,5], Felix von Zweydorf[1], Christian Johannes Gloeckner[1,6], Hannah A. Davies[7,8], Jillian Madine[7,9], Domenico Del Turco[10], Regina Feederle[11,12], Tammaryn Lashley[13,14], Thomas Deller[10], Philipp Kahle[1,5], Jasmin K. Hefendehl[4], Mathias Jucker[1,2], Jonas J. Neher[1,2,#]

[1]German Center for Neurodegenerative Diseases (DZNE), Tübingen, Germany.
[2]Department of Cellular Neurology, Hertie Institute for Clinical Brain Research, University of Tübingen, Tübingen, Germany.
[3]Graduate School of Cellular and Molecular Neuroscience, University of Tübingen, Tübingen, Germany.
[4]Buchmann Institute for Molecular Life Sciences and Institute of Cell Biology and Neuroscience, Goethe University Frankfurt, Frankfurt, Germany.
[5]Laboratory of Functional Neurogenetics, Department of Neurodegeneration, Hertie Institute for Clinical Brain Research, University of Tübingen, Tübingen, Germany.
[6]Core Facility for Medical Bioanalytics, Institute for Ophthalmic Research, Center for Ophthalmology University of Tübingen, Tübingen, Germany.
[7]Department of Cardiovascular and Metabolic Medicine, Institute of Life Course and Medical Sciences, University of Liverpool, U.K.
[8]Liverpool Centre for Cardiovascular Sciences, University of Liverpool, U.K.
[9]Department of Biochemistry and Systems Biology, Institute of Systems, Molecular and Integrative Biology, University of Liverpool, U.K.
[10]Institute of Clinical Neuroanatomy, Dr. Senckenberg Anatomy, Neuroscience Center, Goethe University, D-60590 Frankfurt/Main, Germany
[11]Monoclonal Antibody Core Facility, Institute for Diabetes and Obesity, Helmholtz Zentrum München, Research Center for Environmental Health (GmbH), Neuherberg, Germany.
[12]German Center for Neurodegenerative Diseases (DZNE), Munich, Germany.
[13]Queen Square Brain Bank for Neurological Disorders, UCL Queen Square Institute of Neurology, London, UK.
[14]Department of Neurodegenerative Disease, UCL Queen Square Institute of Neurology, London, UK.
[15]These authors contributed equally to this work.

correspondence should be addressed to:

Dr. Jonas Neher
German Center for Neurodegenerative Diseases
Otfried Müller Str. 23
D-72076 Tübingen, Germany
email: jonas.neher@dzne.de
phone: +49 7071/9254-351

Abstract

Medin is the most common amyloid found in humans, reported to occur in blood vessels of the upper body in virtually everybody over 50 years of age. However, it remains unknown whether deposition of Medin plays a causal role in age-related vascular dysfunction. We now report that aggregates of Medin also develop in the aorta and brain vasculature of wildtype mice in an age-dependent manner. Strikingly, genetic deficiency of the Medin precursor protein, MFG-E8, eliminates not only vascular aggregates but also prevents age-associated decline of cerebrovascular function in mice. Given the prevalence of Medin aggregates in the general population and its role in vascular dysfunction with aging, targeting Medin may become a novel approach to sustain healthy aging.

Significance statement

Vascular dysfunction, as it develops either during normal aging or vascular disease, remains a major medical problem. The amyloid Medin, which is derived from its precursor protein MFG-E8 (through unknown mechanisms), forms insoluble aggregates in the vasculature of virtually anybody over 50 years of age, and it has been hypothesized that Medin aggregation could contribute to age-associated vascular decline; however, mechanistic analyses have so far been lacking. Our data now demonstrate that reminiscent of humans, mice also develop Medin deposits in an age-dependent manner. Importantly, mice that genetically lack Medin show reduced vascular dysfunction in the aged brain. Therefore, the prevention of Medin accumulation should be investigated as a novel therapeutic approach to preserve vascular health in the aging population.

Introduction

Amyloids comprise about 35 identified proteins, which under physiological conditions can convert to insoluble aggregates that are often associated with pathological alterations in the amyloid-containing tissue (1). The most common human amyloid described so far is Medin (also known as AMed), which has been found in ~97% of Caucasians above 50 years of age (2), with Medin deposition found predominantly in the thoracic aorta and other arteries of the upper body (3). Medin has been described as a 50 amino acid long internal fragment of the protein Milk fat globule EGF-like factor-8 (MFG-E8) (4), which itself is best known for its role in the phagocytosis of apoptotic cells but is also required for neovascularization, explaining its localization in blood vessels (5). Under which conditions and how Medin is cleaved from MFG-E8 remains unknown, but its exceedingly high prevalence in the aging population begs the question whether Medin – similar to other amyloids – is associated with tissue dysfunction (6). Of note, previous research suggests that age-associated structural and functional alterations of the arteries contribute to cardiovascular diseases (7) and a role of Medin in promoting age-related vascular dysfunction has been hypothesized based on analyses of human autopsy and post-mortem aorta samples (8–10). Most recently, evidence of increased Medin levels in patients with vascular dementia compared to cognitively unimpaired individuals was also reported (11). However, mechanistic studies and therefore conclusive evidence for a detrimental role of Medin deposition are so far lacking. This is largely because studies on human tissue lack appropriate controls (due to the presence of Medin deposits in virtually all aged human samples) and could therefore only be correlative in nature, and because no animal model for Medin deposition has so far been described that would enable mechanistic analyses.

Therefore, we analyzed here whether Medin deposition also occurs in the vasculature of aging mice. Indeed, we find extracellular Medin aggregates in C57BL/6J mice, with deposition developing in an age-dependent manner. Notably, Medin aggregates are absent in genetically engineered mice that lack the Medin-containing C2 domain of its precursor protein MFG-E8. Moreover, in these Medin-deficient mice, age-associated vascular dysfunction in cerebral arteries is virtually eliminated. Thus, our data provide the first direct evidence for a pathological role of this highly prevalent human amyloid.

Results

MFG-E8/Medin aggregates form in the mouse aorta with age

In humans, Medin aggregates are detectable in blood vessels of the upper body in virtually everyone above the age of 50 (2). While two prior studies in rats and monkeys have reported an increase of aortic levels of the Medin precursor protein MFG-E8 with age (12, 13), it has so far not been investigated whether Medin aggregates are found in other species than humans. Of note, murine and human Medin show 78% amino acid sequence homology (Needleman-Wunsch Global Alignment, BLAST) with the most aggregation-prone region showing high conservation (Fig. 1A) (14, 15). This indicates that mice may be a suitable model to study Medin pathophysiology, although the aggregation propensity of murine Medin may be more limited than its human form (based on TANGO analysis; Fig. 1A).

To assess whether Medin is deposited in the mouse aorta, we collected aorta samples from mice at the age of 2-4, 12 and 20 months. First, we tested whether levels of MFG-E8 increase with age (using a commercial ELISA). Indeed, aorta homogenates showed a significant increase in MFG-E8 protein levels in one-year-old compared to 2-4 months old mice and increased even further in 20-month-old animals (Fig. 1B). Interestingly, at the same time that levels of MFG-E8 increased in the aorta, they decreased in the serum, demonstrating that these changes were not due to blood contamination in the tissue. Immunostaining with a polyclonal antibody against murine MFG-E8, which we found to have high affinity for the C2 and lower affinity for the C1 domain (*SI Appendix*, Fig. S1A and Fig. 1A) confirmed that aortic MFG-E8 staining increases with age (Fig. 1C). Interestingly, MFG-E8 staining revealed irregularly shaped lumps along elastic fibers, reminiscent of findings in human tissue where Medin is found in “nodules and thin streaks” in the aortic media or “irregular clumps” in the intima, and is closely associated with elastic fibers (2). We also confirmed these previous results in human tissue using a new monoclonal anti-human Medin antibody (1H4) (Fig. 1E). While prior studies could not demonstrate that antibodies were specifically detecting Medin, we here ascertained staining specificity by analyzing tissue from mice that lack the Medin-containing C2 domain of MFG-E8 (*Mfge8* C2 KO) (Fig. 1A). In these functional knockout mice, the C2 domain is replaced with a β-galactosidase reporter gene fused to a transmembrane domain. While this does not prevent gene expression, it effectively traps the truncated *Mfge8*/β-galactosidase fusion gene inside the cell, leading to a complete absence of secreted MFG-E8 in *Mfge8* C2 KO animals (as previously confirmed in the aorta and for different cell types; [5, 16, 17] and cp. *SI Appendix*, Fig. S4 for brain tissue). In line with the high affinity of the polyclonal anti-MFG-E8 antibody for the C2 domain (*SI Appendix*, Fig. S1A), staining was absent in the aorta of *Mfge8* C2 KO mice (Fig. 1C) and accordingly, no signal was found in the ELISA for MFG-E8 (Fig. 1B).

To determine whether the observed staining patterns in wildtype mice were indeed due to extracellular aggregates, we next performed immuno-electron microscopy (EM) of aortas from young adult and aged wildtype mice as well as aged *Mfge8* C2 KO mice. As expected from our immunohistochemical analyses, only aged wildtype animals demonstrated immunolabelling, which was found localized on extracellular aggregates (Fig. 1D). While these aggregates appeared amorphous (rather than fibrillar) under EM, these findings demonstrate that MFG-E8 (or its fragments) forms extra-cellular aggregates in an age-specific manner in the mouse aorta.

In humans, aortic Medin deposits can be stained with amyloid-binding dyes such as Methoxy-X04, which we also confirmed here (Fig. 1E; see *SI Appendix*, Table S1 for sample information). In apparent contrast, aggregates in the mouse aorta failed to stain with Methoxy-X04 or Congo Red (*SI Appendix*, Fig. S2). However, in our hands, not all Medin-positive aggregates (stained with anti-human Medin antibody 1H4) in human tissue were stained by amyloid-binding dyes (Fig. 1E; n=3 patients, *SI Appendix*, Table S1 and Fig. S2). Thus, similar to our observations in mice, some Medin deposits in human tissue do not display the characteristic β-sheet structure of other amyloids, possibly representing an earlier aggregation stage.

Aortic deposits in mice show biochemical characteristics of protein aggregates

Given the amorphous appearance of aortic aggregates in aged mice by EM, we wanted to determine whether these deposits shared biochemical features of other aggregated proteins, i.e. protease resistance and insolubility in aqueous media. Therefore, we used a previously published amyloid purification protocol (18) to determine if the aged aorta would contain aggregated proteins. We first tested this protocol using brains of either aged APP23 or APP Dutch transgenic animals. APP23 mice are a model of Alzheimer's disease pathology with widespread parenchymal and vascular amyloid-β deposition (19) while aged APP Dutch animals show amyloid-β deposition restricted to cerebral blood vessels (20). In brief, homogenates were lysed and subjected to iodixanol gradient centrifugation. Samples were then digested with benzonase and proteinase-K (PK) and were subsequently ultracentrifuged to recover the remaining protease-resistant, insoluble material (Fig. 2A). As expected, this procedure yielded enriched monomeric and oligomeric amyloid-β species from the brains of both aged APP23 and APP Dutch animals (*SI Appendix*, Fig. S1B).

Next, we analyzed fresh-frozen aorta samples from human patients, which showed Medin staining by immunohistochemistry (cp. Fig. 1E). In human aorta samples, Western Blotting of the different fractions obtained from the amyloid purification protocol using the monoclonal anti-human Medin antibody (1H4) revealed protein bands corresponding to full-length MFG-E8 but also bands indicating mono- and possibly oligomeric Medin species

(approx. 4, 8 and 12 kDa). After benzonase (P2) and proteinase K (P3) digestion, full-length MFG-E8 and other proteins were degraded, while the protease-resistant material showed distinct bands with molecular weights corresponding to monomeric and oligomeric Medin species as well as a higher molecular weight smear, possibly reflecting higher order aggregates (Fig. 2B).

Analyzing mouse samples next, Western Blotting demonstrated full-length MFG-E8 in the total aorta homogenate (TH) of both young and aged wildtype mice (Fig. 2C; samples are pools of 16 mouse aortas), with significantly stronger signals in the aorta homogenate of aged mice, reflecting our ELISA measurements (Fig. 1B). In contrast, the purification protocol only enriched a protease-resistant MFG-E8-positive fragment from the aorta of aged wildtype mice, while neither young wildtype nor aged *Mfge8* C2 KO aortas yielded MFG-E8 species in the final aggregate-containing fractions (Fig. 2C). Notably, the protease-resistant MFG-E8 fragment in the aged mouse aorta showed a molecular weight of approx. 5 kDa, corresponding to the reported size of Medin (4). These results demonstrate that MFG-E8 fragments, which similar to other protein aggregates are protease-resistant as well as insoluble in aqueous buffers and show a molecular weight that corresponds to the reported size of Medin, accumulate in the aging mouse aorta.

Identification of a Medin-like fragment in the aging mouse aorta

To ascertain that the ~5 kDa band observed by Western Blotting was indeed a Medin-containing peptide, we used a shotgun mass spectrometry approach (Fig. 2D). Briefly, aorta homogenates were pre-fractionated by protein gel electrophoresis and only proteins smaller than ~17 kDa were excised to exclude full-length MFG-E8. First, we verified that we could detect Medin peptides in aggregated material by analyzing recombinant human Medin that had been aggregated *in vitro*. Indeed, following gel electrophoresis and excision of a monomeric as well as an oligomeric band, almost the entire Medin sequence (with the exception of short N- and C-terminal peptides) could be detected by mass spectrometry (*SI Appendix*, Fig. S3).

Next, we compared murine aorta samples (again without further purification procedures) from young and aged wildtype and aged *Mfge8* C2 KO mice. Here, low molecular weight peptides of MFG-E8 (≤17 kDa) were detectable only in aged wildtype aortas. Strikingly, the majority of these peptides could be assigned to the C2 domain and were enriched in the sequence corresponding to the originally reported human Medin (Fig. 2D), also consistent with our epitope mapping of the anti-murine MFG-E8 antibody (Fig. 1A and *SI Appendix*, Fig. S1A). Thus, our mass spectrometry results demonstrate that – similar to observations in human patients – Medin-containing fragments are accumulating in the aging mouse aorta, further corroborating our analyses using immunohistochemistry and biochemical purification approaches.

MFG-E8 and Medin in the aging brain

In humans, Medin deposition has not only been observed in the thoracic aorta but also other larger arteries of the upper body, including basilar and temporal arteries (11, 21, 22) and most recently also arterioles in the brain parenchyma (11). To confirm Medin deposition in cerebral blood vessels, we stained brain sections of aged patients without any major brain diseases (male and female, 80-86 years old; see *SI Appendix*, Table S2 for details) with the anti-human Medin antibody, 1H4. Strikingly, Medin deposits could be seen within and outside the smooth muscle cell layer in leptomeningeal vessels, larger parenchymal vessels and even smaller capillaries, where they also showed aggregate-like morphology (Fig. 3A). Of note, these deposits did not show immunoreactivity for amyloid-β nor were they positive for the amyloid-binding dye Methoxy-X04 (Fig. 3A, *bottom*), in contrast to our findings in the human aorta, where both Methoxy-X04–positive and –negative aggregates were found (Fig. 1E).

Next, we analyzed brain tissue from mice to determine whether cerebral blood vessels would display age-related Medin deposition. Indeed, immunohistochemical staining showed MFG-E8-positive blood vessels in the mouse brain, with more intense and aggregate-like staining being observed in aged animals (Fig. 3B). However, these deposits were again not stained by the classical amyloid-binding dyes Methoxy-X04 and Congo Red (*SI Appendix*, Fig. S2). Nevertheless, an age-related increase in cerebral MFG-E8 protein levels could be observed in wildtype mice by ELISA (Fig. 3C), reflecting our findings in the aorta (Fig. 1). Moreover, semi-automated quantification of smooth muscle actin and MFG-E8 staining in serial brain sections revealed no difference in total vascular coverage but showed an increase of cerebrovascular MFG-E8 staining with age (Figs. 3D/E). Notably, in brain sections from aged *Mfge8* C2 KO animals, we could detect intracellular MFG-E8-positive puncta both in parenchymal as well as vascular cells, reflecting expression and intracellular retention of the truncated *Mfge8*/β-galactosidase fusion protein (*SI Appendix*, Fig. S4A). Accordingly, in brain homogenates from aged *Mfge8* C2 KO animals, the fusion protein appeared as a distinct band ~200 kDa (in line with previous reports [17]), while the band of full-length MFG-E8 observed in wildtype animals was completely absent (*SI Appendix*, Fig. S4B). Thus, our results indicate that in wildtype mice the aorta as well as cerebral blood vessels show age-associated deposition of MFG-E8 (fragments) that are likely to contain Medin.

Lack of MFG-E8 rescues age-associated vascular dysfunction

We wondered whether Medin deposition could contribute to the decline in vascular function, which occurs with age both in mice and humans (23–25). Because age-related changes in regional cerebral blood flow are not detectable by PET/MRI measurements in wildtype animals (26), we assessed cerebral vascular function by 2-photon *in vivo* imaging, which has been

shown to detect age-associated cerebrovascular alterations in mice (27). Here, we analyzed the function of cerebral arterioles in living animals, focusing on the middle cerebral artery (MCA) territory in the sensorimotor cortex, where we also observed Medin deposits in aging mice (Fig. 3F). We triggered increases in blood flow to the hindlimb region by evoking neuronal activity using mechanical hindlimb stimulation (Fig. 3G), a mechanism called functional hyperemia (28, 29). Indeed, in response to hindlimb stimulation, adult animals (6.4±1.1 months old) showed a rapid dilation of arteries followed by a slower constriction; this response was indistinguishable between adult wildtype and *Mfge8* C2 KO animals (Fig. 3G). Importantly, in aged wildtype animals (22.1± 2.4 months old) dilation of the imaged arteries was significantly slower than in adult animals, in line with increased vascular arterial stiffness in aging animals and humans (30, 31). In contrast, both dilation and constriction were significantly improved in aged *Mfge8* C2 KO compared to wildtype animals (Fig. 3G). Thus, our data demonstrate that the lack of Medin improves vascular function in aging animals.

It has been suggested that vascular amyloid may lead to blood vessel dysfunction through toxic effects on smooth muscle cells (22, 32). However, in contrast to previous reports (32), we did not observe overt loss of smooth muscle cells in cerebrovascular regions with Medin deposits (Fig. 3A). Moreover, neither global endothelial cell volume (based on CD31 staining) nor astrocytic endfeet coverage of cerebral blood vessels (based on Aquaporin-4 staining), which is crucial for appropriate neurovascular coupling (24, 29), were affected by aging or in wildtype versus *Mfge8* C2 KO animals (*SI Appendix*, Fig. S5). While we cannot exclude that the lack of MFG-E8 affected other compartments of the brain, our data strongly suggest that accumulation of Medin (or larger MFG-E8 fragments) in amyloid-like deposits contributes to age-related vascular dysfunction in wildtype mice, possibly through affecting vascular elasticity (33).

Discussion

Our data presented here indicate that the most common human amyloid, Medin (or Medin-containing fragments of MFG-E8), also shows age-associated aggregation in wildtype mice and demonstrate a pathogenic role of its accumulation in driving age-associated vascular dysfunction. Strikingly, Medin deposits form in aging mice despite their relatively limited lifespan, reflecting the previous finding that Medin deposits can be found in the vast majority of people over 50 years of age (2). However, in mice, Medin aggregates do not stain with classical amyloid dyes (Congo Red, Methoxy-X04) and appear amorphous by electron microscopy, possibly reflecting their lower (predicted) aggregation propensity (Fig.1A) or indicating an early stage of fibril formation and/or maturation. Interestingly, it has been reported that in human aortic tissue the amount of Medin in its amyloid state is significantly lower in patients with aortic aneurysm or dissection, while non-fibrillar Medin deposits are significantly

higher in the diseased aorta (10) and correlate with reduced aortic elasticity (9). Thus, non-fibrillar forms of Medin could in fact be more pathogenic and notably, we find that Medin deposits in the human brain vasculature do not stain with amyloid dyes. It has been reported that amyloids can exist as structurally distinct "strains" (with different affinity for common amyloid dyes), which propagate through prion-like mechanisms, i.e. through templated misfolding of the native peptide (e.g. [34, 35]). Thus, it is conceivable that different strains of Medin form in the mouse and human vasculature and become (locally) amplified, providing a possible explanation for the differences in amyloid dye affinity observed in our analyses. Further relating to the role of amyloids in vascular dysfunction, it has been shown that soluble amyloid-β monomers and oligomers significantly impair vascular function in Alzheimer's disease (e.g. [36–38]), and it will therefore be important to determine which specific types of Medin aggregates are responsible for inducing vascular dysfunction in the aging brain.

Even though Medin is the most common human amyloid described so far, little is known about its contribution to disease. Correlative analyses of human tissue suggest that MFG-E8 and Medin may contribute to vasculitis and thoracic aneurysms and dissection (9, 10) as well as vascular dementia (11). Mechanistically, it has been hypothesized that Medin amyloid leads to cell toxicity through promoting inflammatory and oxidative stress, thereby altering the arterial wall structure and predisposing arteries to age-related vascular dysfunction and disease (39–42). However, these studies were unable to determine whether Medin aggregates were cause or consequence of pathological vascular changes. Our observation that Medin deposition occurs in murine blood vessels with age and is absent in *Mfge8* C2 KO animals allowed us to examine in living mice whether this process contributes to vascular dysfunction. Our results now provide the first direct evidence that Medin aggregation within (cerebral) blood vessels may be causal for vascular dysfunction. Whether this occurs independently or is interlinked with previously reported mechanisms of age-related cerebrovascular dysfunction (including increases in reactive oxygen species [25]) requires further investigation. Nevertheless, our findings indicate that vascular function can be improved by preventing Medin aggregation. Given the high prevalence of cardiovascular, cerebrovascular, and neurodegenerative diseases in the aging population (43, 44), preservation of vascular function remains a major challenge in medical research (45–47). Targeting Medin aggregation should therefore be investigated as a novel therapeutic option to promote healthy aging of the vasculature. Notably, the NMR structure of the Medin-containing C2 domain of human MFG-E8 has been resolved (PDB 2L9L; [48]); this may allow for rational drug design to prevent Medin aggregation through kinetic stabilization of its native structure, as exemplified for example by recent approaches to prevent transthyretin amyloidosis (49).

Finally, a potential interaction between Medin and amyloids in the brain is also of interest, because amyloidosis is prevalent in many neurodegenerative diseases. Previous

experiments showed that Medin can act as a heterologous seed for the aggregation of serum amyloid A (50), but whether it interacts with other extracellular amyloids and in particular amyloid-β, which deposits both in the parenchyma as well as in blood vessels of the brain, remains unknown. Despite their structural similarities, amyloids do not necessarily co-aggregate and can even show cross-inhibitory effects (51, 52). Therefore, understanding if and how Medin may contribute to age-related amyloidosis in the brain will be investigated in future studies.

Materials and Methods

Human tissue

Ascending aortic tissue samples were obtained from patients undergoing elective aneurysmal repair at Liverpool Heart and Chest Hospital (*SI Appendix*, Table S1). This study was ethically approved by Liverpool Bio-Innovation Hub (project approval reference 15-06 and 18-07). One case (patient 2) was obtained from informed consent post-mortem collection through the Leeds GIFT scheme. Ethical approval for this patient was conferred by NRES Committee East of England-Cambridge South (approval reference 11/EE/0528). Human brain tissue (Supplementary Table S2) was obtained from the Queen Square Brain Bank for Neurological Disorders (UCL Institute of Neurology, London, UK; approval protocol No: EXTMTA5/16).

This study was also approved by the ethical committee of the Medical Faculty, University of Tübingen, Germany (Protocol No: 354/2016BO2). Informed consent was obtained from all participants.

Mice

Male and female C57BL/6J and C57BL/6J-Mfge8 $Gt^{(KST227)Byg}$ mice (5) (generously provided by Dr. Clotilde Théry, INSERM U932, Institute Curie, France), were bred in-house under specific pathogen-free conditions. All experiments were performed in accordance with German veterinary office regulations (Baden-Württemberg and Hessen) and were approved by the local authorities for animal experimentation (Regierungspräsidium) of Tübingen, Germany (Approval numbers: N03/14, N02/15, N07/16, §4MIT v. 05.03.2018, §4MIT v. 18.08.2016) and Frankfurt, Germany (protocol number: FR-1001).

Tissue collection and analyses

For brain and aorta preparation, mice were deeply anesthetized and transcardially perfused with phosphate-buffered saline (PBS) and processed for biochemical analyses and immunostaining as described in *SI Appendix, Materials and Methods*.

2-photon imaging of vascular function

Cranial window surgeries were carried out as previously described in detail (53–55), using hindlimb stimulation to elicit functional hyperemia in the middle cerebral artery territory of the sensorimotor cortex, as described in detail in *SI Appendix, Materials and Methods*.

Statistics

Statistical analysis was performed using Prism 6 and JMP software (version 14.2.0) as indicated in the Figure legends and as described in detail in *SI Appendix, Materials and Methods*. All data shown are means ± S.E.M.

Acknowledgements

We thank Dr. Jörg Odenthal and Carina Leibssle for assistance with animal maintenance and care, Franziska Klose and Karsten Boldt (Core Facility for Medical Bioanalytics, University of Tübingen) for technical help, and Anke Biczysko for expert technical assistance with electron microscopy. This work was supported by grants from the German Research Foundation (DFG) to Jonas Neher (NE 1951/2-1 and -2), and British Heart Foundation to Jillian Madine (FS/12/61/29877). Work in the lab of Jasmin Hefendehl is supported by grants from the German Research Foundation (DFG) (HE 6867/4-1 and 3-1). The graphics in Fig.2A were generated using biorender.com.

Author contributions

Unless otherwise noted, mouse and human tissue analyses were performed by K.D. and J.W., with assistance from K.W; A.J.K. performed analyses of astrocytic endfeet coverage and ELISA for brain homogenates. Specific anti-human medin antibody clones were generated and pre-selected by R.F. Computational analyses were implemented by A.S.; *in vivo* 2P experiments were performed by M.C. and J.K.H.; R.M. and C.R. performed epitope mapping under supervision from P.K.. H.A.D. and J.M. performed recombinant human Medin expression and sourced human aortic tissue. F.v.Z. and C.J.G. performed mass-spec analyses; D.D.T. and T.D. performed EM analyses; T.L. selected and sourced human brain tissue. J.J.N conceived the study and coordinated experiments together with M.J.; J.W. and J.J.N. wrote the manuscript, with contributions from all authors.

Competing interests

The authors have no conflict of interest.

References

1. M. D. Benson, *et al.*, Amyloid nomenclature 2018: recommendations by the International Society of Amyloidosis (ISA) nomenclature committee. *Amyloid* **25**, 215–219 (2018).
2. G. Mucchiano, G. G. 3rd Cornwell, P. Westermark, Senile aortic amyloid. Evidence for two distinct forms of localized deposits. *Am. J. Pathol.* **140**, 871–877 (1992).
3. S. Peng, *et al.*, Medin and medin-amyloid in ageing inflamed and non-inflamed temporal arteries. *J. Pathol.* **196**, 91–96 (2002).
4. B. Häggqvist, *et al.*, Medin: an integral fragment of aortic smooth muscle cell-produced lactadherin forms the most common human amyloid. *Proc. Natl. Acad. Sci. U. S. A.* **96**, 8669–74 (1999).
5. J.-S. Silvestre, *et al.*, Lactadherin promotes VEGF-dependent neovascularization. *Nat. Med.* **11**, 499–506 (2005).
6. D. Eisenberg, M. Jucker, The amyloid state of proteins in human diseases. *Cell* **148**, 1188–1203 (2012).
7. S. S. Najjar, A. Scuteri, E. G. Lakatta, Arterial aging: is it an immutable cardiovascular risk factor? *Hypertens. (Dallas, Tex. 1979)* **46**, 454–462 (2005).
8. T. J. Muckle, Giant cell inflammation compared with amyloidosis of the internal elastic lamina in temporal arteries. *Arthritis Rheum.* **31**, 1186–1189 (1988).

9. H. A. Davies, *et al.*, Idiopathic degenerative thoracic aneurysms are associated with increased aortic medial amyloid. *Amyloid* **26**, 148–155 (2019).
10. S. Peng, *et al.*, Role of aggregated medin in the pathogenesis of thoracic aortic aneurysm and dissection. *Lab. Invest.* **87**, 1195–1205 (2007).
11. N. Karamanova, *et al.*, Endothelial Immune Activation by Medin: Potential Role in Cerebrovascular Disease and Reversal by Monosialoganglioside-Containing Nanoliposomes. *J. Am. Heart Assoc.* **9**, e014810 (2020).
12. Z. Fu, *et al.*, Milk fat globule protein epidermal growth factor-8: A pivotal relay element within the angiotensin II and monocyte chemoattractant protein-1 signaling cascade mediating vascular smooth muscle cells invasion. *Circ. Res.* **104**, 1337–1346 (2009).
13. M. Wang, *et al.*, MFG-E8 activates proliferation of vascular smooth muscle cells via integrin signaling. *Aging Cell* **11**, 500–508 (2012).
14. A.-M. Fernandez-Escamilla, F. Rousseau, J. Schymkowitz, L. Serrano, Prediction of sequence-dependent and mutational effects on the aggregation of peptides and proteins. *Nat. Biotechnol.* **22**, 1302–1306 (2004).
15. A. Larsson, *et al.*, Unwinding fibril formation of medin, the peptide of the most common form of human amyloid. *Biochem. Biophys. Res. Commun.* **361**, 822–828 (2007).
16. K. Atabai, *et al.*, Mfge8 Is Critical for Mammary Gland Remodeling during Involution. *Mol. Biol. Cell* **16**, 5528–5537 (2005).
17. E. F. Nandrot, *et al.*, Essential role for MFG-E8 as ligand for αvβ5 integrin in diurnal retinal phagocytosis. *Proc. Natl. Acad. Sci.* **104**, 12005 LP – 12010 (2007).
18. J. Stohr, *et al.*, Purified and synthetic Alzheimer's amyloid beta (Abeta) prions. *Proc. Natl. Acad. Sci. U. S. A.* **109**, 11025–11030 (2012).
19. C. Sturchler-Pierrat, *et al.*, Two amyloid precursor protein transgenic mouse models with Alzheimer disease-like pathology. *Proc. Natl. Acad. Sci. U. S. A.* **94**, 13287–92 (1997).
20. M. Herzig, D. Winkler, K. Bürki, Abeta is targeted to the vasculature in a mouse model of hereditary cerebral hemorrhage with amyloidosis. *Nat. Neurosci.* **7** (2004).
21. S. Peng, *Medin Amyloid in Human Arteries and its Association with Arterial Diseases* (2006).
22. S. Peng, J. Glennert, P. Westermark, Medin-amyloid: A recently characterized age-associated arterial amyloid form affects mainly arteries in the upper part of the body. *Amyloid* **12**, 96–102 (2005).
23. S. Tarantini, C. H. T. Tran, G. R. Gordon, Z. Ungvari, A. Csiszar, Impaired neurovascular coupling in aging and Alzheimer's disease: Contribution of astrocyte dysfunction and endothelial impairment to cognitive decline. *Exp. Gerontol.* **94**, 52–58 (2017).
24. C. Iadecola, M. Nedergaard, Glial regulation of the cerebral microvasculature. *Nat. Neurosci.* **10**, 1369–1376 (2007).
25. H.-M. Kang, I. Sohn, J. Jung, J.-W. Jeong, C. Park, Age-related changes in pial arterial structure and blood flow in mice. *Neurobiol. Aging* **37**, 161–170 (2016).
26. F. C. Maier, *et al.*, Longitudinal PET-MRI reveals β-amyloid deposition and rCBF dynamics and connects vascular amyloidosis to quantitative loss of perfusion. *Nat. Med.* **20**, 1485–1492 (2014).
27. L. Park, J. Anrather, H. Girouard, P. Zhou, C. Iadecola, Nox2-Derived Reactive Oxygen Species Mediate Neurovascular Dysregulation in the Aging Mouse Brain. *J. Cereb. Blood Flow Metab.* **27**, 1908–1918 (2007).
28. A. Y. Shih, *et al.*, Two-photon microscopy as a tool to study blood flow and neurovascular coupling in the rodent brain. *J. Cereb. Blood Flow Metab.* **32**, 1277–1309 (2012).
29. D. Attwell, *et al.*, Glial and neuronal control of brain blood flow. *Nature* **468**, 232–243 (2010).
30. M. A. Hajdu, D. D. Heistad, J. E. Siems, G. L. Baumbach, Effects of aging on mechanics and composition of cerebral arterioles in rats. *Circ. Res.* **66**, 1747–1754 (1990).
31. P. Anna, *et al.*, Carotid and Aortic Stiffness. *Hypertension* **47**, 371–376 (2006).
32. D. T. Winkler, *et al.*, Spontaneous Hemorrhagic Stroke in a Mouse Model of Cerebral Amyloid Angiopathy. *J. Neurosci.* **21**, 1619 LP – 1627 (2001).
33. A. Larsson, *et al.*, Lactadherin binds to elastin – a starting point for medin amyloid

formation? *Amyloid* **13**, 78–85 (2006).
34. C. Condello, *et al.*, Structural heterogeneity and intersubject variability of Aβ in familial and sporadic Alzheimer's disease. *Proc. Natl. Acad. Sci.* **115**, E782 LP-E791 (2018).
35. J. Rasmussen, *et al.*, Amyloid polymorphisms constitute distinct clouds of conformational variants in different etiological subtypes of Alzheimer's disease. *Proc. Natl. Acad. Sci.* **114**, 13018 LP – 13023 (2017).
36. R. Nortley, *et al.*, Amyloid β oligomers constrict human capillaries in Alzheimer's disease via signaling to pericytes. *Science (80-.).* **365**, eaav9518 (2019).
37. Z. Suo, *et al.*, Soluble Alzheimers β-amyloid constricts the cerebral vasculature in vivo. *Neurosci. Lett.* **257**, 77–80 (1998).
38. K. Niwa, *et al.*, Aβ-peptides enhance vasoconstriction in cerebral circulation. *Am. J. Physiol. Circ. Physiol.* **281**, H2417–H2424 (2001).
39. J. Madine, D. A. Middleton, Comparison of aggregation enhancement and inhibition as strategies for reducing the cytotoxicity of the aortic amyloid polypeptide medin. *Eur. Biophys. J.* **39**, 1281–1288 (2010).
40. H. Chiang, P. Chu, T. Lee, MFG-E8 mediates arterial aging by promoting the proinflammatory phenotype of vascular smooth muscle cells. **0**, 1–14 (2019).
41. M. Wang, H. H. Wang, E. G. Lakatta, Milk fat globule epidermal growth factor VIII signaling in arterial wall remodeling. *Curr. Vasc. Pharmacol.* **11**, 768–776 (2013).
42. R. Q. Migrino, *et al.*, Amyloidogenic medin induces endothelial dysfunction and vascular inflammation through the receptor for advanced glycation endproducts. *Cardiovasc. Res.* **113**, 1389–1402 (2017).
43. S. W. Wen, C. H. Y. Wong, Aging- and vascular-related pathologies. *Microcirculation* **26**, e12463 (2019).
44. World Health Organization, Global Status Report On Noncommunicable Diseases 2014 (2014).
45. J. A. H. R. Claassen, Cognitive decline and dementia: are we getting to the vascular heart of the matter? *Hypertens. (Dallas, Tex. 1979)* **65**, 505–506 (2015).
46. M. P. Pase, *et al.*, Association of Aortic Stiffness With Cognition and Brain Aging in Young and Middle-Aged Adults: The Framingham Third Generation Cohort Study. *Hypertens. (Dallas, Tex. 1979)* **67**, 513–519 (2016).
47. J. C. de la Torre, Cerebral hemodynamics and vascular risk factors: setting the stage for Alzheimer's disease. *J. Alzheimers. Dis.* **32**, 553–567 (2012).
48. H. Ye, *et al.*, NMR solution structure of C2 domain of MFG-E8 and insights into its molecular recognition with phosphatidylserine. *Biochim. Biophys. Acta - Biomembr.* **1828**, 1083–1093 (2013).
49. M. M. Alhamadsheh, *et al.*, Potent Kinetic Stabilizers That Prevent Transthyretin-Mediated Cardiomyocyte Proteotoxicity. *Sci. Transl. Med.* **3**, 97ra81 LP-97ra81 (2011).
50. A. Larsson, S. Malmström, P. Westermark, Signs of cross-seeding: Aortic medin amyloid as a trigger for protein AA deposition. *Amyloid* **18**, 229–234 (2011).
51. T. Bachhuber, *et al.*, Inhibition of amyloid-beta plaque formation by alpha-synuclein. *Nat. Med.* **21**, 802–807 (2015).
52. J. Coomaraswamy, *et al.*, Modeling familial Danish dementia in mice supports the concept of the amyloid hypothesis of Alzheimer's disease. *Proc. Natl. Acad. Sci.* **107**, 7969 LP – 7974 (2010).
53. J. K. Hefendehl, *et al.*, Long-term in vivo imaging of β-amyloid plaque appearance and growth in a mouse model of cerebral β-amyloidosis. *J. Neurosci.* **31**, 624–629 (2011).
54. J. K. Hefendehl, *et al.*, Repeatable target localization for long-term in vivo imaging of mice with 2-photon microscopy. *J. Neurosci. Methods* **205**, 357–363 (2012).
55. P. Füger, *et al.*, Microglia turnover with aging and in an Alzheimer's model via long-term in vivo single-cell imaging. *Nat. Neurosci.* **20**, 1371–1376 (2017).

Figure Legends

Commented [JN1]: Delete Figures before submission.

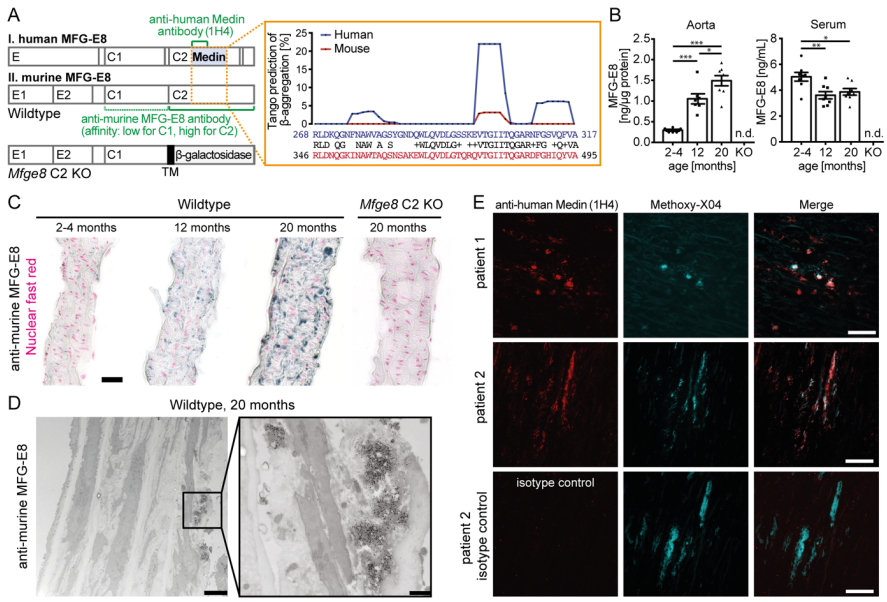

Figure 1: MFG-E8-positive aggregates accumulate in the mouse aorta with age.

A, *Left*, Schematic structure of human and murine MFG-E8 showing the major protein domains and highlighting protein regions recognized by the two antibodies used throughout this study (green). The structure of the truncated *Mfge8* gene in the C2 domain knockout mice is shown at the bottom, indicating the introduction of a β-galactosidase reporter gene fused to a transmembrane domain (TM), which effectively traps the gene product inside the cell. *Right*, Amino acid sequence comparison of the reported human Medin sequence with the homologous murine sequence; *top*: TANGO prediction of aggregation-prone peptides within the Medin sequence, with high conservation but lower aggregation propensity in the mouse. **B**, Protein levels in wildtype mouse aorta and serum in young adult (2-4 months old; n_{aorta}=3/3, n_{serum}=5/3 female/male), adult (12-month-old, n_{aorta}=3/4, n_{serum}=3/5 female/male) and aged (20-month-old, n_{aorta}=3/5, n_{serum}=3/5 female/male) animals and *Mfge8* C2 knockout tissue (n = 1/1 female/male). Data shown are means ± S.E.M., with one-way ANOVA for aorta: $F(2,18)=29.97$, $P<0.0001$; serum: $F(2,21)=6.85$, $P=0.005$; */**/*** indicate $P<0.05/0.01/0.001$ for posthoc Tukey test. **C**, Representative immunohistochemical staining for MFG-E8 (black) and cell nuclei (red) of 5 µm sections of the mouse aorta in wildtype and *Mfge8* C2 KO animals. **D**, Immuno-electron microscopy for MFG-E8 of aged wildtype mouse aorta (n=2 female mice; 24-month-old); no aggregates were found in young adult (n=2 male; 3-month-old) or aged *Mfge8* C2 KO (n=1/1 male/female; 21-23 months old) animals. **E**, Staining of human aorta sections (5 µm) with anti-human Medin antibody (clone 1H4) or an isotype-control antibody (bottom row) and the amyloid-binding dye Methoxy-X04. Scale bars are 25 µm in C, 2500 nm (low magnification image) and 500 nm (high magnification image) in D and 25 µm in E. 'n.d.', not detectable.

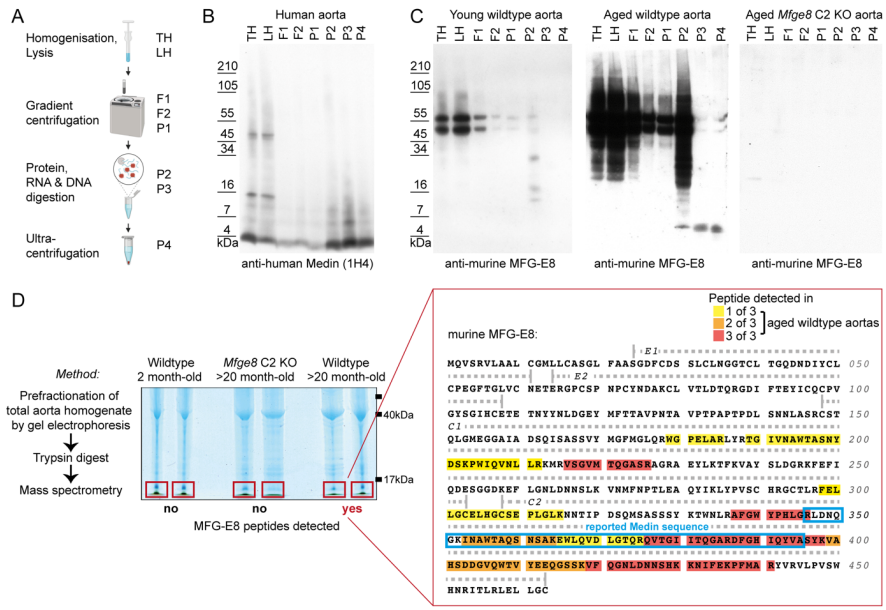

Figure 2: Aortic deposits in mice show biochemical characteristics of protein aggregates and are enriched in Medin-containing fragments of MFG-E8.

A, Graphical summary of the purification procedure for the enrichment of protein aggregates from tissue homogenates. **B**, Analysis of human aorta homogenates (total homogenate: TH; lysed homogenate: LH) reveals enrichment of Medin-positive bands, corresponding to monomeric (~4 kDa) and oligomeric (~8/12 kDa) species. **C**, In mouse aorta samples (pools of 16 aortas were used as input), full-length MFG-E8 is degraded and a ~5 kDa fragment is enriched only from aged wildtype but not young wildtype or aged *Mfge8* C2 KO aortas. **D**, Mass spectrometry (MS) analysis of total aorta homogenate of young adult wildtype (2-month-old; n=1/1 female/male) and aged (20-month-old) *Mfge8* C2 KO (n=2 females) and wildtype (n= 1/2 female/male) mice. Following pre-fractionation and in-gel digestions, gel sections containing small proteins (<17 kDa) were excised and subjected to MS analysis. No MFG-E8 peptides were found in samples from young wildtype or aged *Mfge8* C2 KO animals while aged wildtype aortas contained ≤17 kDa fragments of MFG-E8, which were most consistently found in the C2 domain (color-code indicates detection in different number of samples; yellow/orange/red = 1/2/3 out of 3 samples). The reported human Medin sequence is highlighted with a blue frame.

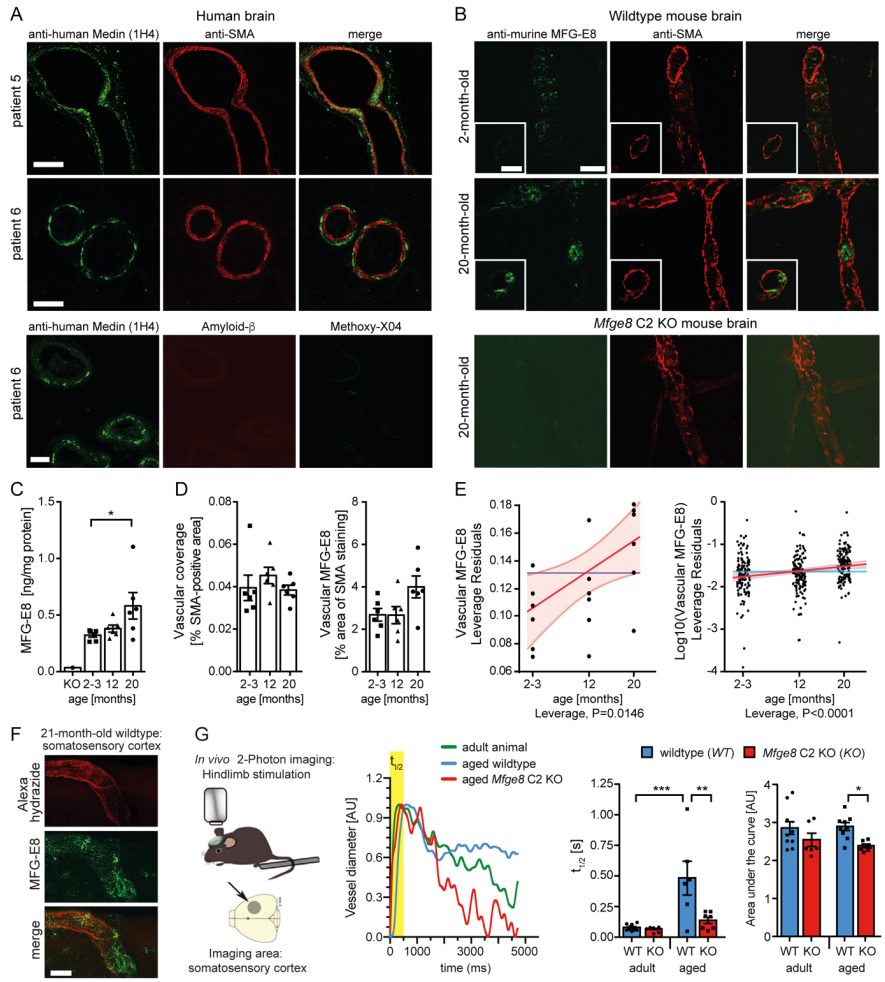

Figure 3: **MFG-E8/Medin deposition causes age-associated cerebrovascular dysfunction.**

A, In brain sections of healthy human patients (n=3 patients analyzed) extensive vascular staining of aggregate-like structures is seen with a monoclonal anti-human Medin antibody (1H4). Aggregates are largely localized in the tunica media and the parenchymal side of the vessels. *Bottom*, Medin-positive deposits do not stain with the amyloid-dye Methoxy-X04 and are negative for amyloid-β. Scale bar: 50 µm. **B,** In aged (20-month-old) but not young (2-month-old) mice, aggregate-like structures are also present in the brain vasculature, where they are found mostly in the tunica media and the luminal side of blood vessels. Scale bar: 25 µm. **C**, Quantification of total MFG-E8 protein levels with age in the wildtype mouse brain (n=3/3 females/males per group, significant Kruskal-Wallis test: KW statistic=5.93, P=0.047, followed by Dunn's posthoc comparison, * P<0.05). **D**, Quantification of the overall vascular

density (area of smooth muscle actin, *SMA*, staining) and vascular MFG-E8 staining (% MFG-E8 staining within SMA-positive area) in brain sections with age in wildtype mice (n=3/3 females/males per group). Data shown are means ± S.E.M. **E**, Regression analysis for the impact of age on cerebrovascular accumulation of MFG-E8/Medin (effect leverage plot, where a least squares line [red] and confidence bands [shaded red] are fitted). Analysis for the mean vascular MFG-E8 staining per animal (*left*) and per brain section (*right*). **F,** Representative confocal z-stack of an artery from the middle cerebral artery territory in the somatosensory cortex (horizontal brain section; Scale bar: 25 µm). **G**, Schematic illustration of *in vivo* analysis of vascular function in the brain of living mice using 2-photon imaging of functional hyperemia. **H**, *left*, Representative traces and *right*, quantification of the change in diameter of individual arterioles in adult wildtype (n=4; 5/6/6/6-month-old male) or *Mfge8* C2 KO (n=3; 6/6/8-month-old male) and aged wildtype (n=4; 21/22/22/22-month-old male) or *Mfge8* C2 KO (n=3; 19/22/27-month-old male) animals, with $t_{1/2}$ reflecting the speed of vessel dilation, and the area under the curve reflecting the speed of constriction (1-3 arterioles per animal). Arterial dilation and constriction are significantly improved in aged *Mfge8* C2 KO compared to aged wildtype animals. Two-way ANOVA; $t_{1/2}$: significant main effects of age*genotype/genotype/age: $F(1,25)=7.763/9.369/16.15$, $P=0.01/0.0052/0.0005$; Area under the curve: significant main effect of genotype, $F(1,28)=8.62$, $P=0.0066$; */**/*** $P<0.05/0.01/0.001$ for posthoc Bonferroni comparisons. Data shown are means ± S.E.M. (data points are measurements from individual blood vessels).